JOURNAL OF MATERIALS SCIENCE 30 (1995) 1480–1486

Polyacetal and thermoplastic polyurethane elastomer toughened polyacetal: crystallinity and fracture mechanics

G. KUMAR, N. R. NEELAKANTAN, N. SUBRAMANIAN
Department of Chemical Engineering, Indian Institute of Technology, Madras-600 036, India

The effect of thermoplastic polyurethane (TPU) elastomer on the melting point and the percentage crystallinity of polyacetal (POM) is studied by differential scanning calorimetry (DSC). Wide angle X-ray diffraction (WAXD) scans of POM, TPU and their blends have been taken and the results indicate that the crystalline structure of POM remains unaffected even after the addition of amorphous TPU. The influence of defects like holes and notches on the ultimate tensile strength has been examined. The resistance to crack initiation (J_c), the resistance to steady state crack propagation (R_p) and the resistance to crack growth at maximum load (R_{max}) are estimated. The POM/TPU blends display higher crack resistance values than pure POM. The hysteresis energy of blends is determined and is found to increase with TPU content.

1. Introduction

The technology of polymer blends has developed into an important segment of polymer science in the past two decades. Additionally, the utility of polymer blends has increased significantly and is expected to continue. With the advent of melt-processable thermoplastic elastomers, the horizons of polymer blends have been widened from plastic–plastic systems to plastic–rubber ones, with toughness improvement of engineering plastics receiving the major emphasis. A small amount of discrete rubber particles in a plastic can greatly improve the crack and impact resistance of normally brittle plastic. The toughening of general-purpose plastics, such as polystyrene and PVC, has contributed considerably to the growth of the plastics industry. More important, the toughening of high-performance plastics, such as polyacetals, aromatic polyesters, and nylon, has provided second-generation materials that can outperform most classic construction materials [1].

Polyacetal (polyoxymethylene, POM) is a semi-crystalline engineering thermoplastic of considerable commercial importance. However, POM is extremely brittle in notched impact, restricting its range of engineering applications. Therefore, POM is toughened with thermoplastic polyurethane (TPU) elastomer in order to widen its scope of applications into areas where it ought to have a high degree of impact strength. Flexman *et al.* [2] developed POM compositions containing 5–40% TPU with an increased melt strength, a decreased crystallization rate, and increased and more consistent die swell for blow moulding applications. Flexman [3] also compared the impact resistance of toughened polyacetal and the base resin and suggested some aspects of its fracture mechanism.

Chang and Yang [4] investigated POM toughening with TPU elastomer in terms of rheological, mechanical and morphological properties. John *et al.* [5] studied the effects of elongation rate and determined fracture mechanics parameters such as strain energy release rate, G, Rice's contour integral, J, and fracture toughness, K, under plane stress conditions for POM/TPU blends. Kloos and Wolters [6] reported that the notched impact strength of impact-modified POMs containing urethane rubber increased with decreasing particle size of the dispersed TPU. Robert *et al.* [7] disclosed POM/TPU compositions with enhanced impact resistance even at low temperatures suitable for making exterior automobile body parts, from a mixture of oxymethylene copolymer and polyurethane.

The objectives of the present work are: (i) to study the effect of addition of TPU elastomer on the percentage crystallinity and crystalline structure of POM, (ii) to investigate the influence of defects like holes and notches on the ultimate tensile strength of both POM and the blends, (iii) to determine the crack resistance values, and (iv) to estimate and compare the hysteresis values of POM and the blends.

2. Experimental procedure

2.1. Materials

POM, used in this study, is an injection moulding grade copolymer (Celcon M-140) obtained from Hoechst Celanese, USA. ^{13}C nuclear magnetic resonance (CNMR) reveals that this copolymer contains

0022–2461

2–3% oxyethylene repeat units, the remainder being oxymethylene [8]. TPU elastomer, Estane 58311, is of commercial type and was supplied by B. F. Goodrich Co., Belgium. It is a polyether-based TPU compound with a weight average molecular weight (M_w) of 1.5×10^5.

2.2. Procedure

The TPU elastomer and POM were melt-mixed in appropriate ratios using a 30 mm single-screw extruder ($L/D = 20$) with a screw speed of 50 r.p.m. A special mixing head was used for this purpose. Temperatures ranging from 170 to 200 °C were employed depending upon the needs of the individual formulations. After extrusion, the material was granulated. POM blends containing 10, 20 and 30% TPU are denoted as AU91, AU82 and AU73, respectively, in this study.

A Dupont 910 differential scanning calorimeter was used to study the melting behaviour of POM and the blends. About 10 mg of each sample was melted at 200 °C for at least five minutes and then cooled to 30 °C to allow the polymer to crystallize under the same thermal condition. At this point the sample was reheated at 5 °C min^{-1} to 200 °C. The melting point was observed and recorded. The melting enthalpy was calculated by integrating the area under the melting endotherm of the DSC trace using the software provided with the instrument. The crystallinity (X_c) of POM in the blend was computed according to

$$X_c = \left(\frac{\Delta H}{\Delta H^\circ}\right) \times 100\% \quad (1)$$

where $\Delta H^\circ = 326$ J g^{-1} is the fusion enthalpy of POM of 100% crystallinity [9]. ΔH is the enthalpy of POM in the blend.

Wide angle X-ray diffraction (WAXD) analysis of POM, TPU and their blends were obtained with RICH-SEIFERT XRD 3000P X-ray diffractometer, Germany (CuK_α-radiation; monochrome). The accelerating voltage and electric current used were 35 kV and 30 mA, respectively. Blends of different composition for WAXD analysis were obtained by hot-pressing the samples at 195 °C and allowing them to cool to room temperature at a rate of 4 °C min^{-1}.

An injection moulding machine was used for making samples for fracture mechanics studies. To evaluate the influence of defects present in the materials, holes and side notches of various notch parameters were created in the tensile test specimens and load deflection curves were obtained [5]. For this fracture study, dumbbell shaped test specimens of the dimensions $150 \times 14 \times 1.5$ mm were made. The notch parameters used are: (1) $2r/w$, 0.128, 0.143, 0.157, and 0.171 and (2) a/w, 0.0714, 0.143, 0.214, and 0.286, where r is the radius of the hole which is drilled at the middle of the specimens, w is the width and a is the notch length of the razor cut specimens. A crosshead speed of 5 mm min^{-1} was employed using a Zwick universal testing machine (UTM, 1465).

The fracture mechanics parameters, critical energy for crack initiation (J_c), resistance to steady state crack growth (R_p), and resistance to crack growth at maximum load (R_{max}), were determined using the three-point bend method developed by Kim and Joe [10, 11]. The specimens measured 120, 14 and 5 mm for length, width, and thickness, respectively. For this study, samples with different notch lengths from 1 to 4 mm were made with a sharp razor to avoid crazing and crack branching. The distance between the two supports was 80 mm and the loading rate was 5 mm min^{-1}. The load versus load-point deflection curves were obtained using the Zwick UTM 1465 for further analysis.

Hysteresis tests were carried out by loading to a predetermined load level and then returning at the same speed. The tests were performed on the same type of samples which were utilised for stress concentration studies. A constant crosshead speed of 2.0 mm min^{-1} and different loading levels of 200, 175, 150, and 125 N were applied using the Zwick UTM 1465.

3. Results and discussion

3.1. Crystallinity

DSC analysis was carried out to measure the melting point, enthalpies of fusion, and thereby the percentage crystallinity of POM and its blends with TPU. DSC was performed on the POM and the blends in order to examine the effect that the added TPU exert on the melting behaviour of the semi-crystalline POM. DSC thermograms, showing the crystalline melting endotherms, are presented for POM and the blends in Fig. 1. The results are summarized in Table I. The enthalpies of fusion of POM upon heating at constant rate decrease as TPU is added. Table I also shows the percentage crystallinity [12] which has been calculated from the melting enthalpies after normalizing for the POM content of the blend. The percentage crystallinity of POM decreases as the TPU content in the blend increases [13]. At the same time, the melting point of POM is affected only marginally. Thus it can be concluded that crystallization in POM is impeded to some extent due to the presence of the amorphous TPU component.

3.2. Crystalline structure

The X-ray diffraction scans of the POM/TPU blends as a function of Bragg angle (2θ) at room temperature are displayed in Fig. 2. POM and the blends give a sharp crystalline peak and about three small peaks in the region of the Bragg angle (2θ) between 10° and 70°, indicating their semi-crystalline nature. The XRD peak of TPU illustrates its amorphous nature. The strong diffraction peak in POM is located at the diffraction angle (2θ) of 23.38. It is noticed that the incorporation of TPU does not alter the crystal structure of the POM at all, judging from the fact [14] that the four intensity peaks of POM in the blends are observed in the same Bragg angles in all the cases. It is also exemplified from the fact that the d-spacings of POM crystal planes do not vary much with TPU as seen in Table II. As the positions of peak maximum

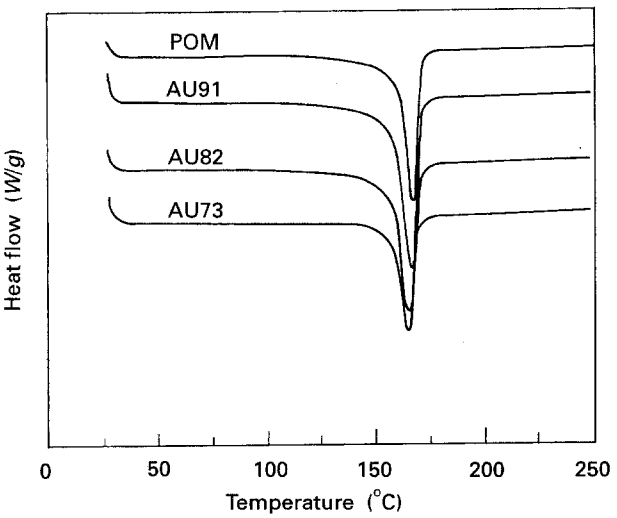

Figure 1 DSC melting endotherms of POM and POM/TPU blends.

TABLE I DSC analysis of POM and the blends

Blend sample	T_m (°C)	H_f (J/g) (based on total weight)	H_f (J/g) (based on POM weight)	Crystallinity (%)
POM	166.9	166.3	166.3	51.0
AU91	166.3	143.1	159.0	48.8
AU82	165.2	120.4	150.5	46.2
AU73	164.1	91.5	130.7	40.1

are independent of the composition, it becomes clear that the unit cell dimensions of POM remain unchanged [15].

Apparent crystallite size (ACS), which is a measure of both the size of the crystallites and the degree of crystalline imperfection, is determined from the full-width at half-maximum $\Delta_{(2\theta)}$ of the crystalline peaks using the Scherrer equation [16].

$$\text{ACS} = 0.9\lambda(\Delta_{(2\theta)}\cos\theta)^{-1} \quad (2)$$

where λ is the wavelength (0.1542 nm) and 2θ is the position of the peak maximum. As seen from Table II, the ACS of blends is lower than that of the pure POM. This suggests that the growth of the crystallites is inhibited in the blends compared to that in pure POM. Such lower crystallinity and smaller or imperfect crystallites might contribute towards improved fracture toughness/impact strength of the blends [16].

3.3. Stress concentration due to defects

Design of engineering components requires sound understanding about the fracture behaviour of the materials under loads at various conditions. In conventional design, the material is assumed to be defect-free, and design practices do not consider prevention of failure initiation at the defects, or imperfections that will be inherently present or caused in all materials, either during fabrication or in service. So the nature of the original flaw and its subsequent behaviour under load are of importance. If the flaw is

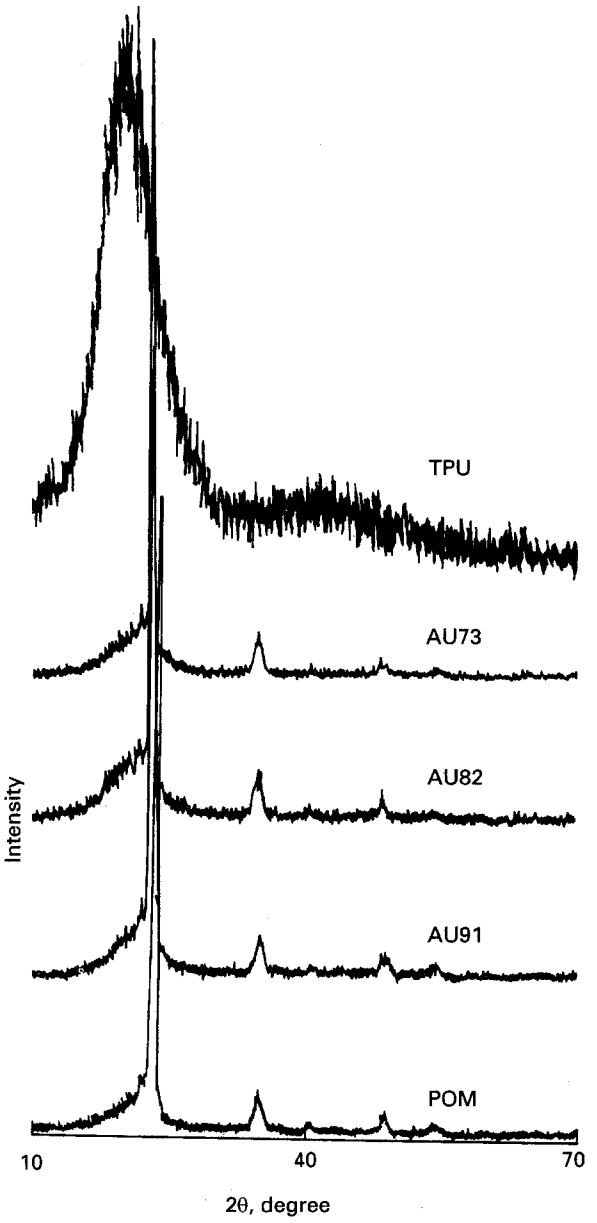

Figure 2 X-ray diffraction scans of POM, TPU and their blends.

TABLE II WAXD analysis of POM and the blends

Blend sample	FWHM	2θ	*d*-spacings POM-crystal planes (nm)	ACS (nm)
POM	0.524	23.280	0.38179	15.4728
AU91	0.531	22.942	0.38162	15.2597
AU82	0.570	23.314	0.38199	14.2254
AU73	0.580	23.436	0.37927	13.9831

small, it is possible that most of the life may be spent in an initiation phase or the flaw may not grow at all and in certain cases this could be controlled by yielding and crazing mechanisms. So if flaw size and its behaviour are known, a safe working stress may be arrived at [5]. A component with a defect may not fail immediately on loading, but may experience a stable crack growth before final failure. If the load is kept

below a certain value, the crack may not grow at all. Hence, it may be of immense importance if one can predict the load at which instability sets in when defects are present in structures.

It is well known that stress concentration due to defects can adversely alter the strength of the materials. The load deflection curves for POM and AU73 with holes of various notch parameters are given in Fig. 3. It is clear that the stress concentration produced by the holes reduced the strength and stiffness in all cases. Similar effects were exhibited by side-notched specimens in tensile strength and these results are presented in Fig. 4. From the above results, breaking strength based on nominal area (P/wt where P is the load at break, w the width and t thickness of the sample) is determined for both notched and unnotched specimens. Their ratios are calculated and presented as a function of notch parameters $2r/w$ or a/w as the case may be. This type of representation of material behaviour in a non-dimensional form will be useful to designers. The results are displayed in Fig. 5. Results demonstrate that a hole of particular diameter present in a material is less critical than a notch of the same dimension [5]. This is due to the high stress intensity at the notch tip. When holes are present up to a notch parameter of about 0.14, the strength is almost equal to that of an unnotched specimen. A further increase in hole diameter results in more reduction in strength. A similar reduction in strength is observed with side-notched specimens and the reduction starts even at the low values of a/w. Fig. 5 also

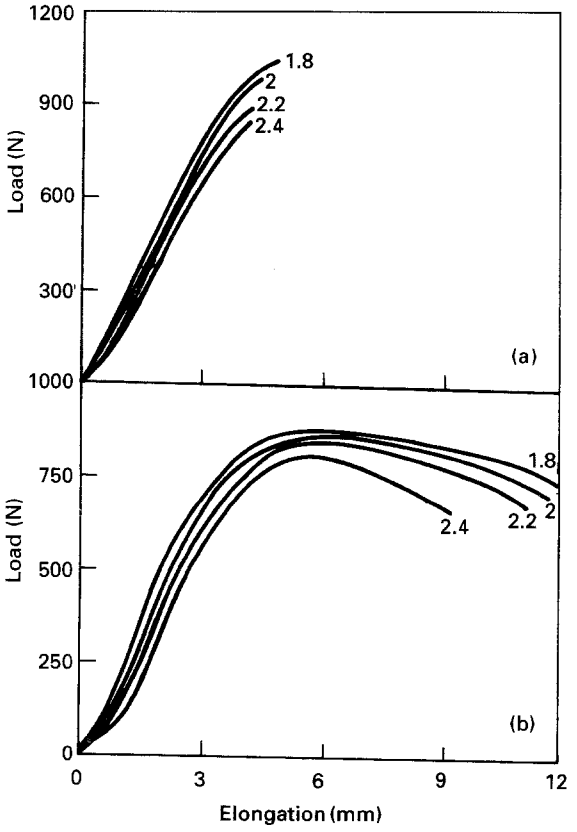

Figure 3 Effect of holes on tensile strength for (a) POM and (b) AU73. Hole diameters in mm are shown on the corresponding curves.

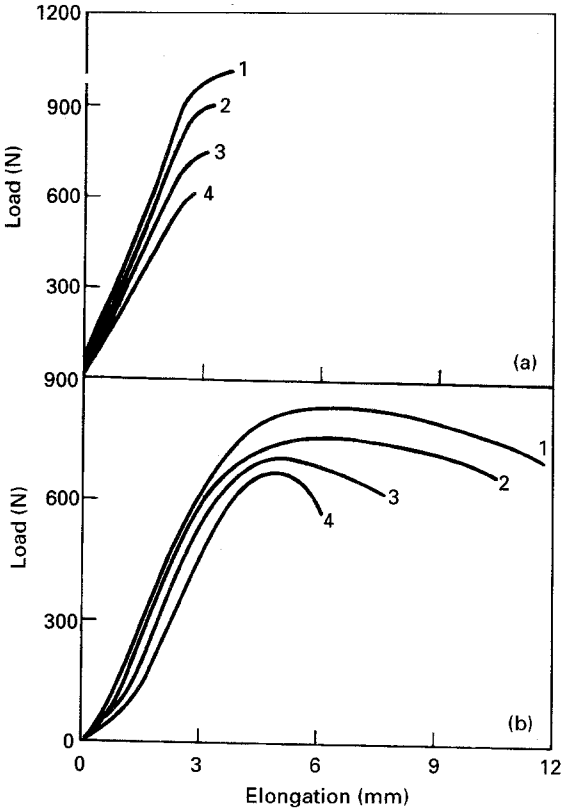

Figure 4 Effect of notches on tensile strength for (a) POM and (b) AU73. The notch lengths in mm are shown on the corresponding curves.

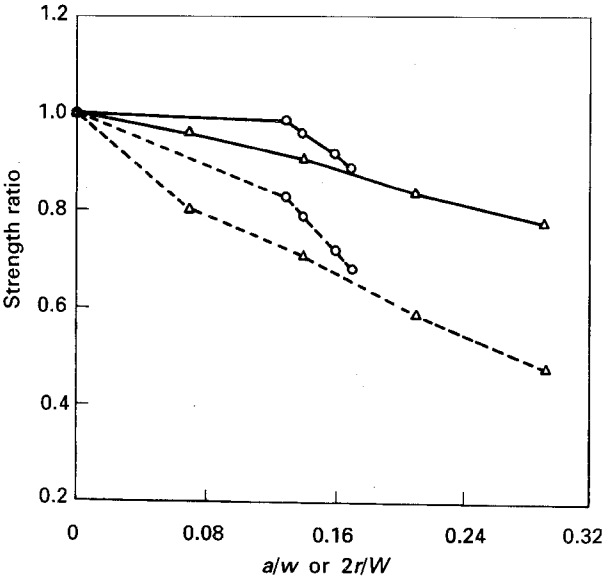

Figure 5 Relative strength based on crack parameters for notch/hole parameters for POM and AU73. ○, hole; △, notch; ——, AU73; – – –, POM.

reveals that the strength retention is greater in the case of AU73 when compared to that of the POM. This indicates that the addition of elastomer helps in reducing the notch sensitivity of POM.

3.4. Crack resistance of blends

In the present study, the fracture mechanics values were obtained using a technique developed by Kim

and Joe [10, 11] which has previously been used successfully on less complex polymeric materials. Their work has resulted in a simple method for determining crack resistance values. Otterson *et al.* [17] investigated the effects of compatibilizer level on the fracture mechanics values (J_c, R_p, and R_{max}) of a nylon 6/ABS polymer blend using this technique. The crack initiation resistance can be found in terms of the critical J-integral value (J_c) utilising the locus line of crack initiation points (measured using a compound microscope) on load-displacement records. It has been shown that J_c can be computed from the following equation

$$J_c = -\frac{1}{B}\frac{\Delta U_c}{\Delta a} \quad (3)$$

where B is the sample thickness, a is the initial crack length, and U_c is the essential energy required to initiate the crack. It is possible to determine the resistance to crack growth at maximum load (R_{max}) using the maximum load points on the load versus load point deflection curves as characteristic points. Determination of an R_{max} value depends upon whether or not the complete load versus deflection curve (R curve) exhibits a point of sharp curvature between the initiation and steady state resistance.

$$R_{max} = -\frac{1}{B}\frac{\Delta U_L}{\Delta a} \quad (4)$$

where U_L is the area surrounded by the locus line of maximum load points, the load versus load-point deflection curve, and the x-axis. The resistance to steady state crack propagation (R_p) is determined in a similar way using the formula

$$R_p = -\frac{1}{B}\frac{\Delta U_f}{\Delta a} \quad (5)$$

where U_f is the total energy for fracture. The detailed procedure to determine the above parameters has been described in [17].

Fig. 6 shows typical load versus load-point deflection curves obtained for POM and AU73 using three-point bending. Crack initiation points are shown as black dots on each curve. The total energy required to initiate the crack (U_c) was determined and plotted in accordance with Equation 3 for the set of specimens in which crack initiation could be observed. The resulting plots for POM and TPU are given in Fig. 7. The slopes of each of these plots represent J_c for each material and these values are given in Table III.

The total energy up to maximum load (U_L) for each specimen was determined and plotted in accordance with Equation 4. These plots are also shown in Fig. 8(a). The slopes of these plots represent R_{max} for each material and these values are provided in Table III.

The total energy for fracture (U_f) for each specimen was determined and plotted in accordance with Equation 5. These plots are shown in Fig. 8(b). The slopes of these plots represent R_p for each material and these values are given in Table III.

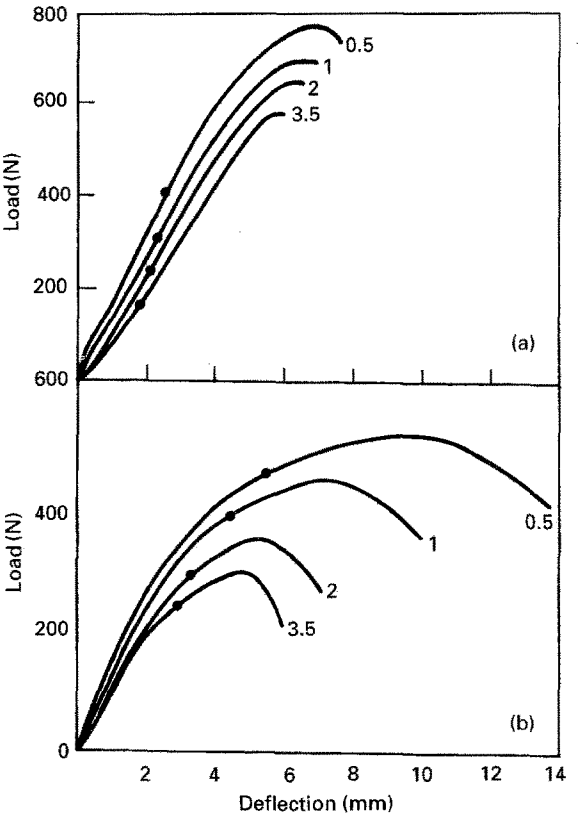

Figure 6 Three-point bending test using various precracked samples of (a) POM and (b) AU73. The crack lengths in mm are shown on the corresponding curves.

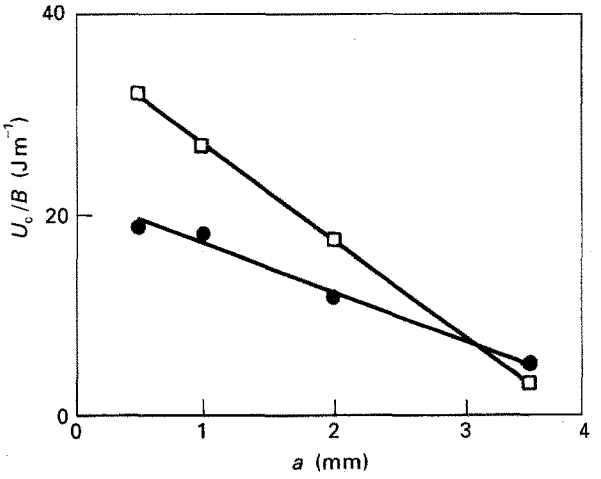

Figure 7 U_c/B versus initial crack length for POM (●) and AU73 (□).

TABLE III Crack resistance values for POM and the blend AU73

Crack resistance	POM	AU73
J_c (kJ m^{-2})	4.8	9.5
R_{max} (kJ m^{-2})	11.2	14.7
R_p (kJ m^{-2})	12.3	34.1

It is seen that the addition of 30% TPU has increased the crack resistance values substantially. The blend AU73 has the crack initiation resistance (J_c) twice that of the POM. While there is only a marginal rise in R_{max} value, there is a tremendous increase in J_c

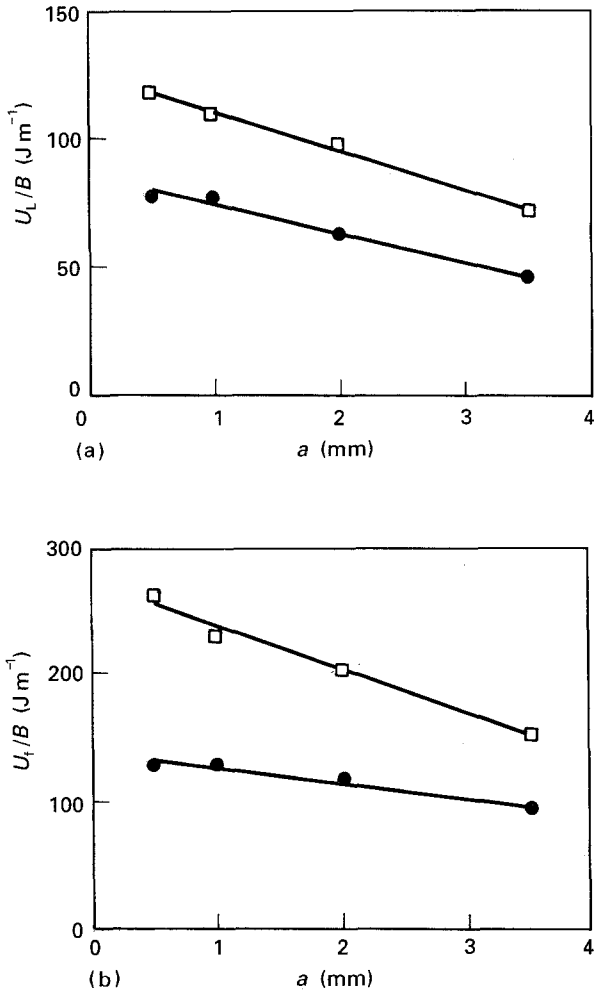

Figure 8 (a) U_L/B versus initial crack length and (b) U_f/B versus initial crack length for POM (●) and AU73 (□).

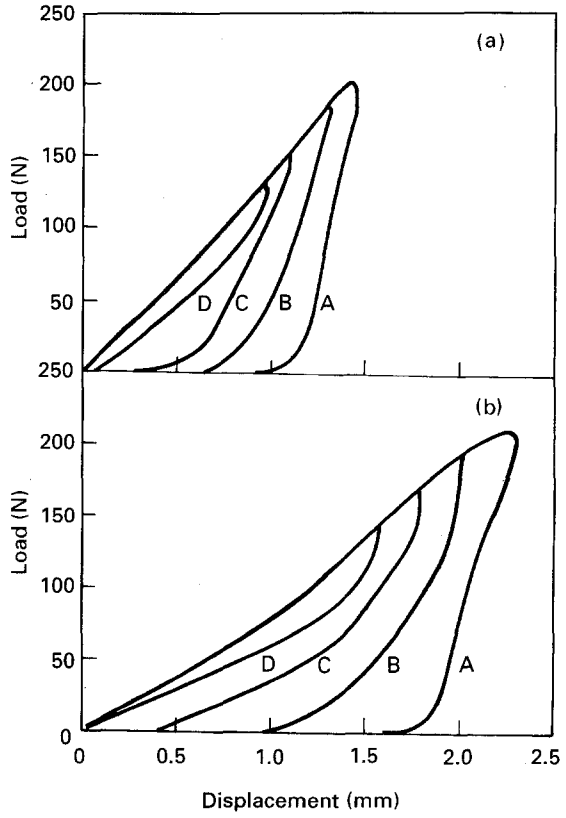

Figure 9 Hysteresis curves at different loading levels for (a) POM; (b) AU73. A = 200 N, B = 175 N, C = 150 N, D = 125 N.

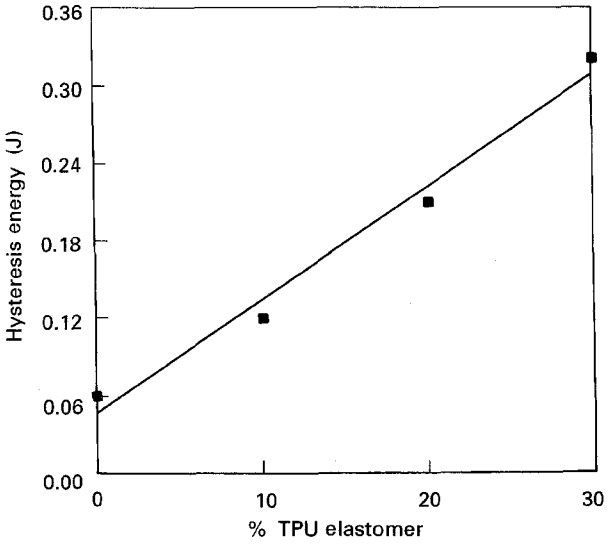

Figure 10 Effect of TPU content on the hysteresis energy of POM/TPU blends. Load = 200 N.

and R_p values for the blend containing 30% TPU. The higher resistance value of blend is indicative of its improved crack resistance.

3.5. Hysteresis

Hysteresis is defined as the energy dissipated in the strain cycle where the unloading path is below the loading path. Strictly speaking, hysteresis can be applied only when the deformed material returns to its original shape (i.e. zero strain). The hysteresis or the loss energy can be calculated from the energy difference between the input and the recovery in a cyclic loading and unloading process [18]. Fig. 9 shows the hysteresis curves of POM and AU73. This reveals that higher load levels lead to higher percentage of hysteresis energy [4] in both POM and the blend AU73. It is observed from Fig. 10 that the hysteresis energies of the blends increase monotonically as the TPU content in POM increases from 0 to 30%. This trend is almost synonymous with the impact strength suggesting that the increase of hysteresis energy may also be taken as an approximate measure of improvement in toughness/impact strength [18].

4. Conclusions

The percentage crystallinity of POM in the blends decreases as the TPU content increases. WAXD reveals that the incorporation of amorphous TPU does not change the crystal structure of POM. The reduction in ultimate tensile strength due to a notch is found to be larger than that due to a hole of the same diameter. The POM/TPU blends are less notch-sensitive when compared to pure POM. The addition of TPU to POM enhances the crack resistance values substantially. The hysteresis energy increases when TPU is added to POM, possibly signifying the improvement in toughness.

Acknowledgements

The authors thank Mr K. Ramakrishnan, Materials Science Research Centre, Indian Institute of Technology, Madras, for helpful discussions and assistance in obtaining the X-ray scans.

References

1. R. B. SEYMOUR, "Rubber Toughened Plastics", edited by C. K. Riew (American Chemical Society, Washington, DC, 1989).
2. European Patent, 121, 407 (1984); U.S. Patent, 479, 942 (1983).
3. E. A. FLEXMAN, Jr., *Mod. Plast.* February (1985) 72.
4. F. C. CHANG and M. Y. YANG, *Polym. Engng Sci.* **30** (1990) 543.
5. R. JOHN, N. R. NEELAKANTAN and N. SUBRAMANIAN, *Polym. Engng Sci.* **32** (1992) 20.
6. F. KLOOS and E. WOLTERS, *Kunststoffe* **75** (1985) 735.
7. U. S. Patent, 625, 954 (1984); European Patent, 167, 369 (1986).
8. J. M. MACHADO and R. N. FRENCH, *Polymer* **33** (1992) 439.
9. B. WUNDERLICH, "Macromolecular Physics, volume-3: Crystal Melting" (Academic Press, New York, 1980).
10. B. H. KIM and C. R. JOE, *Polym. Test.* **7** (1987) 355.
11. *Idem, Engng Fract. Mech.* **34** (1) (1989) 221.
12. C. J. ONG and F. P. PRICE, *J. Polym. Sci., Symp.* **63** (1978) 45.
13. W. Y. CHIANG and M. S. LO, *J. Appl. Polym. Sci.* **36** (1988) 1685.
14. C. S. HA and S. C. KIM. *J. Appl. Polym. Sci.* **35** (1988) 2211.
15. D. J. IHM, C. S. HA and S. C. KIM, *Polymer (Korea)* **12** (1988) 249.
16. N. S. MURTHY, H. MINOR, M. K. AKKAPEDDI and B. VAN BUSKIRK, *J. Appl. Polym. Sci.* **41** (1990) 2265.
17. D. M. OTTERSON, B. H. KIM and R. E. LAVENGOOD, *J. Mater. Sci.* **26** (1991) 1478.
18. C. B. LEE and F. C. CHANG, *Polym, Engng Sci.* **32** (1992) 792.

Received 22 October 1993
and accepted 5 September 1994